

# Reconstruction of Ionic Single-Channel Currents Based on Hidden Markov Model

Xiaoyan Qiao

College of Physics and Electronics Engineering  
Shanxi University  
Taiyuan, China  
e-mail: xyqiao@sxu.edu.cn

Jinzh Wu, Youer Dong

College of Physics and Electronics Engineering  
Shanxi University  
Taiyuan, China  
e-mail: wjzyigeshagua@163.com

**Abstract**—Single ion channel signal of cell membrane is a stochastic ionic currents in the order of picoampere (pA). Because of the weakness of the signal, the background noise always dominates in the patch-clamp recordings. The threshold detector is traditionally used to eliminate noise and restore the single channel signal. However, this method cannot work satisfactorily when signal-to-noise ratio is lower. An approach based on hidden Markov model (HMM) is used to reconstruct ionic single-channel currents and estimate model parameters under white background noise. Firstly, ionic single-channel currents were depicted and analyzed by HMM. Then, an iterative algorithm of Baum-Welch was introduced to train HMM and estimate the model parameters. Finally, the ideal channel currents were reconstructed by Viterbi algorithm. Compared HMM with the threshold detection by computer simulating under different transition probabilities and signal-to-noise ratios, and the results have shown that the method performs effectively under the low signal-to-noise ratio (SNR<5.0) and has fast model parameter convergence, high restoration precision and strong noise robustness.

**Keywords**—ionic single-channel currents; hidden Markov model; computer simulating; signal reconstruction

## I. INTRODUCTION

HMM is a signal processing tool with strong time-series modeling, so the HMM theory has been widely used in the speech signal recognition and biomedical signal processing [1-2]. The ion channel of cell membrane is special protein molecules spanning the membrane of excitable cells. In the protein molecule there exists a pore, which, in certain conformations, keeps open and allows the passage of selected ions along the electrochemical gradient to form ionic currents in the order of picoampere. In the other conformations, the pore keeps closed and no currents exist. The former and latter are respectively defined as "open" and "close" of channel, which are related to the transmembrane voltage, the mechanical pressure and neurotransmitter. The patch-clamp technique can record the ionic single-channel currents [3]. However, single-channel patch-clamp recordings are invariably contaminated by background noise. In order to discover the unknown channels to study the kinetic characters of ion channel as well, it is necessary to accurately restore the channel currents from patch-

clamp recordings. Generally, ionic signal-channel currents are detected by half-amplitude threshold detection for idealizing the channel current signal [4]. However, this method cannot work satisfactorily when signal-to-noise ratio is lower. In this case, this method fails completely. This paper is based on the analysis of ionic channel gating mechanism. Furthermore, the HMM is applied to reconstruct the ionic channel currents. In this method, a forward-backward algorithm was used to calculate the probability, and according to the Baum-Welch re-estimation formula, the HMM model parameters were trained and estimated. On this basis, the ideal channel currents were reconstructed by Viterbi algorithm from the contaminated data. Finally, this paper compares HMM with the threshold detection method by computer simulating and analyses the iteration times for algorithm, the reconstructed errors for currents under different transition probabilities and signal-to-noise ratios. The results have shown that the method performs effectively under the low signal-to-noise ratio.

## II. HMM ANALYSE OF IONIC SINGLE-CHANNEL SIGNAL

### A. HMM parameter and algorithm analysis

HMM is a dual stochastic process. One is Markov chain, which is used to describe the transitions between states. The other is stochastic process, which is used to describe the statistical relationship of the states and observed values [5]. The parameters are elucidated as follows:

- $Q = (q_1, q_2 \dots q_N)$  is a state set for Markov chain in which  $N$  denotes the number of states. In this paper, it represents the number of channel current amplitude levels. Usually,  $N=2$  or  $3$ .  $s_t$  denotes the state at time  $t$ .  $S_T = (s_1, s_2 \dots s_T)$ .
- $\pi = (\pi_1, \pi_2 \dots \pi_N)$  is initial state probability. Where,  $\pi_i = P(s_1 = q_i)$ ,  $1 \leq i \leq N$ .
- $A = (a_{ij})_{N \times N}$  is state transition probability matrix. Where,  $a_{ij} = P(s_{t+1} = q_j / s_t = q_i)$ ,  $i, j = 1, 2 \dots N$ .
- $Y_T = (y_1, y_2 \dots y_T)$  is an observed sequence, which is sampled from patch-clamp recordings by computer in the paper.  $T$  is the length of sampling.  $1 \leq t \leq T$ .

- $B = (b_j(y_i))$  is probability density matrix of observed values. Where,  $b_j(y_i) = P(y_i/s_i = q_i)$ , the probability of observed  $y_i$  while the state being  $q_j$  at time  $t$ .  $1 \leq j \leq N$ .

Therefore, HMM can be described as a parameter set  $\lambda = (\pi, A, B, Q)$ . There are three correlative HMM questions when model  $\lambda$  and observed sequence  $Y_T$  are known.

- Given  $\lambda$  and  $Y_T$ , seek the probability  $P(Y_T/\lambda)$ .
- Given  $\lambda$  and  $Y_T$ , seek  $r = (r_t(i))$ . Where,  $r_t(i) = P(s_t = q_i/Y_T, \lambda)$ . And obtain the most likely state sequence.
- Given  $\lambda$  and  $Y_T$ , reestimate parameter  $\lambda^* = (\pi^*, A^*, B^*, Q^*)$  and seek optimal model parameter  $\lambda^{ML}$ , where, ML denotes maximum likelihood estimation.

The fundamental methods to solve above three questions are forward-backward algorithm, Viterbi algorithm and Baum-Welch algorithm [6].

### B. HMM description of ionic single-channel signal

Ionic single-channel currents appear quantal in nature, and have the characteristic of “all” or “none”. They are one by one rectangle, with invariable current amplitude and stochastically variable dwell-times. Though the single-channel currents have only two current amplitude levels, which respectively correspond to the open and close of channel, the channel kinetics has multi open or closed states of different mean dwell-times (corresponding to different open or closed conformations), which take on the same open or closed current levels. This is called the “aggregation” of ion channel conformations. The states are connected by certain way, and the transition between all states is a first-order, finite state and continuous time Markov process [7]. Ionic single-channel currents become the discrete time sequence after sampling by patch-clamp technology. Due to the aggregation of the channel conformations and the background noise from patch-clamp system, the Markov feature of state transition cannot be observed directly. Therefore, HMM is adopted to describe the patch-clamp recordings, which are sum of ion currents and background noise.

### III. THE RECONSTRUCTION OF IONIC SINGLE-CHANNEL SIGNAL

That reconstructing currents from contaminated patch-clamp recordings is to determine an optimal state sequence  $s_1, s_2, \dots, s_{T-1}, s_T$  according to the given patch-clamp recordings  $Y_T$  and model  $\lambda$ . Assuming patch-clamp recordings is  $Y_T = (y_1, \dots, y_t, \dots, y_T)$ , the probability  $P(Y_T/\lambda)$  can be calculated by the forward-backward algorithm. At time  $t$  ( $1 \leq t \leq T$ ), namely:

$$P(Y_T/\lambda) = \sum_{i=1}^N \alpha_i(i) \beta_i(i) \quad (1)$$

Where,  $\alpha_i(i)$  is forward variable and  $\beta_i(i)$  is backward variable.

To avoid “underflow” phenomena in calculation, a proportion factor is added in the forward-backward algorithm [8].

For forward variable:

Initialization:

$$\alpha_1(i) = \pi_i b_j(y_1) \quad \alpha_1^*(i) = \alpha_1(i) / \sum_{i=1}^N \alpha_1(i) \quad (2)$$

Recursion:

$$\alpha_{t+1}^{\#}(j) = [\sum_{i=1}^N \alpha_t^*(i) a_{ij}] b_j(y_{t+1}) \quad 1 \leq j \leq N, 1 \leq t \leq T-1 \quad (3)$$

End:

$$\alpha_{t+1}^*(j) = \alpha_{t+1}^{\#}(j) / \sum_{j=1}^N \alpha_{t+1}^{\#}(j) \quad (4)$$

For backward variable:

Initialization:

$$\beta_T(i) = 1 \quad \beta_T^*(i) = 1 \quad (5)$$

Recursion:

$$\beta_t^{\#}(i) = \sum_{j=1}^N a_{ij} b_j(y_{t+1}) \beta_{t+1}^*(j) \quad (6)$$

End:

$$\beta_t^*(i) = \beta_t^{\#}(i) / \sum_{j=1}^N \alpha_{t+1}^{\#}(j) \quad 1 \leq i \leq N, 1 \leq t \leq T-1 \quad (7)$$

Then, the kinetics parameter  $\lambda^* = (\pi^*, A^*, B^*, Q^*)$  is estimated by the re-estimation formula to make probability  $P(Y_T/\lambda^*)$  maximum. Baum-Welch re-estimation formula is as follows and its deduction sees reference literature [9].

$$\pi_i^* = r_1(i) \quad a_{ij}^* = \frac{\sum_{t=1}^{T-1} \xi_t(i, j)}{\sum_{t=1}^{T-1} r_t(i)} \quad q_i^* = \frac{\sum_{t=1}^{T-1} r_t(i) y_t}{\sum_{t=1}^{T-1} r_t(i)} \quad (8)$$

Let

$$\xi_t(i, j) = \frac{\alpha_t^*(i) a_{ij} b_j(y_{t+1}) \beta_{t+1}^*(j)}{\sum_{i=1}^N \alpha_t^*(i) \beta_t^*(i)}, r_t(i) = \frac{\alpha_t^*(i) \beta_t^*(i)}{\sum_{i=1}^N \alpha_t^*(i) \beta_t^*(i)} \quad (9)$$

Accordingly, parameter  $B^*$  is revised correspondingly:

$$b_i^*(y_i) = P(y_i | s_i = q_i^*) = \frac{1}{\sigma_w \sqrt{2\pi}} \exp\left(-\frac{(y_i - q_i^*)^2}{2\sigma_w^2}\right) \quad 1 \leq i \leq N \quad (10)$$

Where,  $\mu$  and  $\sigma_w^2$  are mean and variance of Gaussian white noise,  $q_i^*$  is the estimated states. The last parameter values are correlative to the initial parameter values. In this paper, the different initial parameters are selected and performed iterative calculation respectively. Then, by comparing the likelihood function of parameters, the global maximal value is selected.

Then Viterbi algorithm is exploited to determine the most likely state sequence. To avoid “underflow” questions, logarithmic processing technology is adopted. The algorithm proceeds as follows:

Initialization:

$$\delta_1(i) = \log[\pi_i] + \log[b_i(y_1)], \varphi_1(i) = 0, 1 \leq i \leq N, 1 \leq t \leq T \quad (11)$$

Recursion:

$$\varphi_t(j) = \arg \max_{1 \leq i \leq N} [\delta_{t-1}(i) + \log a_{ij}] \quad (12)$$

$$\delta_t(j) = \arg \max_{1 \leq i \leq N} [\delta_{t-1}(i) + \log a_{ij}] + \log[b_j(y_t)], 1 \leq j \leq N, 2 \leq t \leq T \quad (13)$$

End:

$$P^*(Y_T / \lambda) = \max_{1 \leq i \leq N} [\delta_T(i)], S_T^* = \arg \max_{1 \leq i \leq N} [\delta_T(i)] \quad (14)$$

Reconstructing state sequences:

$$s_t^* = \varphi_{t+1}(s_{t+1}^*), t = T-1, T-2, \dots, 1 \quad (15)$$

#### IV. SIMULATING EXPERIMENTS AND ANALYSE OF RESULTS

##### A. Compared HMM with the threshold detection method

At first, a total of 2000 samples are generated to describe a sequence of Gaussian white noise from patch-clamp recordings, namely  $\{\omega_t\}$ . Noise mean is 0pA and standard deviation is 1pA. As shown in Figure 1. This background noise is applied in all experiments in the paper.

Then, a Markov sequence  $\{s_t\}$  of 2000 samples is simulated, which is generated from a two-state model with

current amplitude levels 0pA and 3pA, state transition probability  $a_{11}=a_{22}=0.95$ ,  $a_{12}=a_{21}=0.05$ , and length of sampling  $T=2000$ ,  $N=2$ ,  $Q=(0\text{pA}, 3\text{pA})$ ,  $\text{SNR}=3.0$ . As shown in Figure 2. Patch-clamp recordings  $\{y_t\}$  was simulated by noise  $\{\omega_t\}$  superposing to signal  $\{s_t\}$ . As shown in Figure 3.

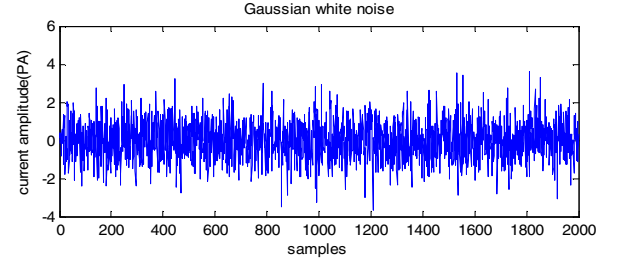


Figure 1. A simulative Gaussian white noise

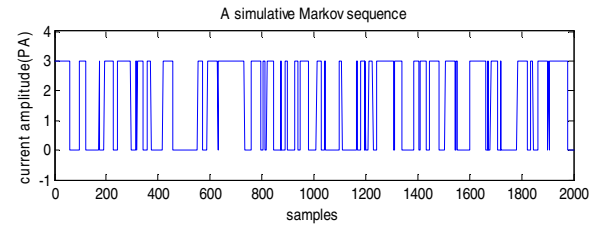


Figure 2. A simulative Markov sequence  $\{s_t\}$

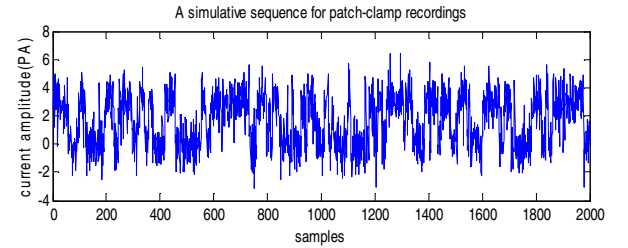


Figure 3. A simulative sequence for patch-clamp recordings  $\{y_t\}$

Firstly, the threshold detection method is adopted to reconstruct the ionic single-channel currents. The threshold value is set to 1.5pA. The current signal of reconstruction is shown in Figure 4. ER denotes error rate, which is defined the ratio of the samples restored falsely and the length T of sampling sequence. In this experiment, ER is 14.65%.

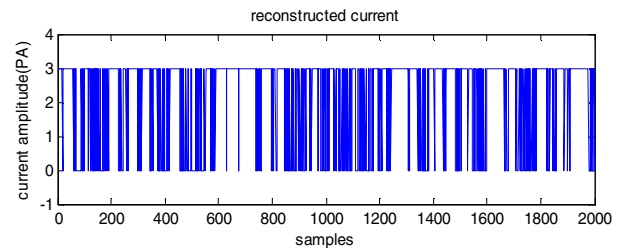


Figure 4. A reconstructive current sequence using the threshold detection

Assuming that initial state transition probability  $a_{11}=a_{22}=0.60$ ,  $a_{12}=a_{21}=0.40$ ,  $\pi_1=\pi_2=0.5$ ,  $a_t(i)$  and  $\beta_t(i)$  are calculated utilizing forward-backward algorithm. Then,

calculate  $A^*$  and  $\pi^*$  by Baum-Welch re-estimation formula. Finally, the ideal current amplitude sequence  $\{s_i^*\}$  is reconstructed by Viterbi algorithm. The result is shown in Figure 5.

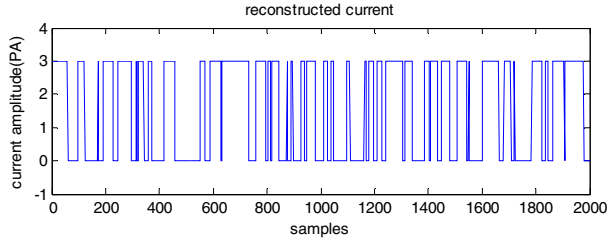


Figure 5. A reconstructive current sequence using HMM

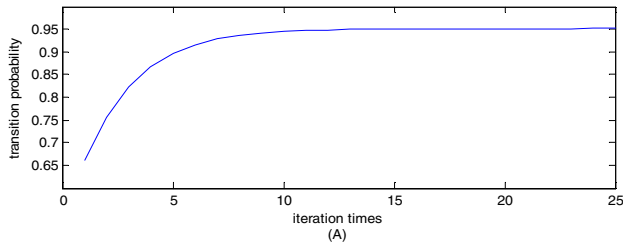
The algorithm converges by 25 iteration times, and  $a_{11}=0.9438, a_{22}=0.9591$ . ER=0.85%. The errors mainly appear on the samples which signal  $\{s_i\}$  sharply change from 0pA to 3pA or contrarily. So HMM is not sensitive to the mutation in the signal. In addition, under the same transition probability, the sequences of patch-clamp recordings with three different SNR (5.0、2.0、1.0) are restored by HMM and the threshold detection method. The error ratio is shown in table 1. The results show that the threshold detection method can't arrive to the demand (ER<10%) of the patch-clamp technique when SNR is lower than 5.0. However, HMM works effectively when SNR is 1.0, so HMM has strong anti-noise capacity.

TABLE I. THE COMPARISON OF PRECISION FOR HMM AND THRESHOLD DETECTION UNDER THE DIFFERENT SNR

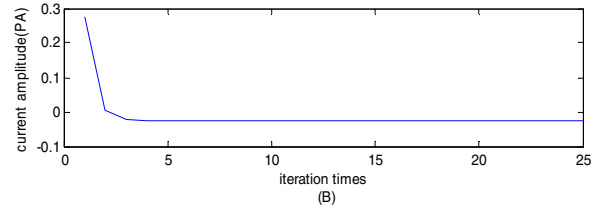
SNR \ ER	the threshold detection method	HMM
SNR=5.0	7.05%	0.20%
SNR=3.0	14.65%	0.85%
SNR=2.0	18.1%	3.05%
SNR=1.0	29.9%	8.70%

#### B. Experimental results under the different SNR

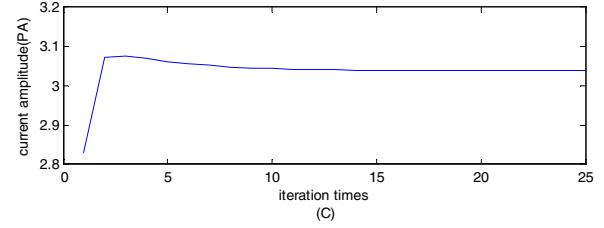
In this experiment, SNR is set as 1.0、2.0、3.0、5.0, through changing the current amplitude of the sequence. The length of sequence is still 2000 samples, transition probability is 0.95, initial state transition probability  $a_{11}=a_{22}=0.60$ ,  $a_{12}=a_{21}=0.40$ ,  $\pi_1=\pi_2=0.5$ . In the case of SNR=3.0, the results are shown in the Figure 6.



(A) Transition probability



(B) The first state



(C) The second state

Figure 6. Convergence processing of transition probability and states under SNR=3.0

The figure shows the algorithm converges by 25 iteration times when SNR is 3.0, and  $a_{11}=0.9438, a_{22}=0.9591, q_1=0.0237, q_2=3.0396$ . In additional, the results under other SNR are shown in the table 2. The experimental results have shown that the error ratio and the iteration times are increased along with the SNR lowering.

TABLE II. THE SIMULATING RESULTS UNDER THE DIFFERENT SNR

SNR	ER(%)	$a_{11}$	$a_{22}$	W	$q_1$	$q_2$
1	8.70	0.9412	0.9518	78	-0.0104	1.0408
2	3.05	0.9578	0.9480	33	-0.0386	1.9984
3	0.85	0.9438	0.9591	25	-0.0237	3.0396
5	0.20	0.9505	0.9610	21	0.0032	4.9959

Note: W denotes the iteration times;  $q_1$  and  $q_2$  denote states respectively.

#### C. Experimental results under the different transition probability

In this experiment, the transition probabilities are 0.93、0.95、0.97, the others are the same as above experiments. The results are shown in table 3. When the transition probability  $a_{ii}$  increases, the error ratio is lower and the iteration times is increased. Due to the transition among states becomes less along with the transition probability  $a_{ii}$  is increased, namely, the mutation among states changes decreased. Therefore, the reconstructive precision improves.

TABLE III. THE SMULATING RESULTS UNDER THE DIFFERENT TRANSITION PROBABILITIES

$a_{ii}(i=1, 2)$	ER(%)	$a_{11}$	$a_{22}$	W	$q_1$	$q_2$
0.93	1.65	0.9352	0.9404	24	0.0041	3.0163
0.95	0.85	0.9438	0.9591	25	-0.0237	3.0396
0.97	0.50	0.9587	0.9785	30	0.0459	2.9514

Note: W denotes the iteration times;  $q_1$  and  $q_2$  denote states respectively.

## V. CONCLUSIONS

In this paper, HMM is simulated to solve ion-channel parameters' estimation and signal reconstruction under white background noise ( $\text{SNR} < 5.0$ ). And the different simulating results are obtained through setting the different parameters. These results have shown that HMM is superior to the threshold detection method under the lower signal-to-noise ratio. The model has the fast convergence, high precision of restoration, and strong noise robustness. Therefore, the model can be used to reconstruct ion single-channel currents under the strong background noise.

## REFERENCES

- [1] K. Q. Wang, "The Application of HMM in Speech Recognition," *Computer Knowledge and Technology*, vol. 34, pp. 1966, December 2008.
- [2] Niranjan P. Bidargaddi, Madihu Chetty and Joarder Kamruzzaman, "Hidden Markov Models Incorporating Fuzzy Measures and Integrals for Protein Sequence Identification and Alignment," *Genomics, Proteomics & Bioinformatics*, vol. 6, pp. 98-103, February 2008.
- [3] X. Y. Qiao, G. Li, L. Lin, "Signal Restoration and Parameters' Estimation of Discrete HMM Based on Stochastic Relaxation," *Chinese Journal of Biomedical Engineering*, vol. 26, pp. 517-518, August 2007.
- [4] John F. Beausang, Chiara Zurla, and Carlo Manzo, "DNA Looping Kinetics Analyzed Using Diffusive Hidden Markov Model," *Biophys J*, vol. 92, pp. 64-69, January 2007.
- [5] D. P. Tan, P. Y. Li, and X. H. Pan, "Application of Improved HMM Algorithm in Slag Detection System," *Journal of Iron and Steel Research, International*, vol. 16, pp. 3-6, January 2009.
- [6] Eddy. SR, "Profile Hidden Markov Model", *Bioinformatics*, vol. 14, pp. 755-63, September 1998.
- [7] F. Qin, "Restoration of Single-Channel Currents Using the Segmental K-Means Method Based on Hidden Markov Modeling," *Biophys J*, vol. 86, pp. 1488-1489, March 2004.
- [8] Y. B. Liu, "Correcting Underflow of Speaker-Recognition Based on Hidden Markov Model," *Control & Automation*, vol. 22, pp. 293-294, July 2006.
- [9] S. P. Du, "The Parametric Estimation of MHMM," *Journal of Anhui University*, vol. 29, pp. 4-6, September 2005.